Noise-Enhanced Multistability in Coupled Oscillator Systems

Seunghwan Kim,* Seon Hee Park, and Chang Su Ryu
Research Department, Electronics and Telecommunications Research Institute,
P.O. Box 106, Yusong-gu, Taejon 305-600, Korea
(Received 7 October 1996)

We study nonequilibrium phenomena in a globally coupled oscillator system with a third harmonic pinning force in the presence of an additive noise and a fluctuating interaction. The system shows a subcritical saddle-node bifurcation from an asymmetric state to a symmetric state at a critical noise intensity leading to multistable states. The fluctuating interaction increases the critical noise intensity and thus enhances the multistability drastically. We show phase diagrams and discuss the nature of the phase transition. [S0031-9007(97)02587-8]

PACS numbers: 05.45.+b, 02.50.Ey, 05.40.+j, 05.70.Fh

Noise effect on a dynamical system has been studied extensively in the context of equilibrium and nonequilibrium phenomena. The study of phase transition, originally limited to equilibrium systems, was extended to nonequilibrium systems [1]. While an additive noise provides equilibrium phenomena such as a disordering effect and a symmetry-breaking transition, a multiplicative noise coupled to the state of the system induces nonequilibrium phenomena such as a change of the stability of the system. The multiplicative noise remains the focus of current research [1–3]. The question of the interplay between multiplicative and additive noises in the systems has also been raised continuously [3,4]. While second-order transition induced by the multiplicative noise has been studied [1,5], its effect on first-order transition remains to be investigated.

In this paper we study the effect of the multiplicative noise on the multistability investigating the nonequilibrium phenomena of the globally coupled oscillator systems with a third harmonic pinning force subject to a fluctuating interaction and an additive noise. It is shown that the additive noise and the fluctuating interaction induces a subcritical saddle-node bifurcation from an asymmetric state to a symmetric state at a critical noise intensity leading to multistable states. The fluctuating coupling increases the critical noise intensity and thus enhances the multistability drastically. We show phase diagrams and discuss the nature of the phase transition.

In the presence of additive and multiplicative noises, a model of N coupled oscillators with a third harmonic pinning force under study is expressed by the Langevin equation

$$\frac{d\phi_i}{dt} = -\, b\sin(3\phi_i) - \frac{K}{N}[1 + \sigma_M \eta_i(t)] \times \sum_{j=1}^{N} \sin(\phi_i - \phi_j) + \sigma_A \xi_i(t)\,, \qquad (1)$$

where ϕ_i, $i = 1, 2, \ldots, N$, is the phase of the ith oscillator. On the right-hand side of Eq. (1) the first term is a third harmonic pinning force, and the second term describes global coupling which depends on the phase difference of two oscillators with fluctuating interaction. $\xi_i(t)$ and $\eta_i(t)$ are independent Gaussian white noises characterized by

$$\langle \xi_i(t)\rangle = \langle \eta_i(t)\rangle = \langle \xi_i(t)\eta_j(t')\rangle = 0\,,$$
$$\langle \xi_i(t)\xi_j(t')\rangle = \langle \eta_i(t)\eta_j(t')\rangle = 2\delta_{ij}\delta(t - t')\,,$$

and σ_A and σ_M measure the intensities of the additive noise and fluctuating interaction, respectively. Throughout this paper we set $K = 1$ using a suitable time unit.

Equation (1) is invariant under the global finite translation

$$\phi_i \to \phi_i + \frac{2\pi}{3} \qquad (2)$$

for all ϕ_i's and under the global inversion $\phi_i \to -\phi_i$ for all ϕ_i's. In the absence of the noises the system has three stable fixed points synchronized perfectly at 0, $2\pi/3$, and $4\pi/3$, respectively. The stable fixed points are related by the symmetry operation (2). For small additive noise, the system fluctuates near the fixed points implying that in the large-N limit, the phase space divides into three ergodic components related by the symmetry operation (2) and that the system remains in a ergodic component given initially leading to the asymmetric state. The ergodic components merge into an ergodic whole phase space for large additive noise restoring the symmetry and thus leading to a phase transition. Numerical simulations show that the global finite translation symmetry is broken at small additive noise intensity. The global inversion symmetry, however, persists regardless of the additive and multiplicative noise intensities with the initial condition which belongs to the ergodic component including the fixed point $\phi_i = 0$ for all i. For the other initial conditions the system has the symmetry of the global inversion following the global translation.

The macroscopic behavior of the system can be described by the probability distribution $P(\{\phi_i\}, t)$ of ϕ_i's at time t, whose evolution is governed by the Fokker-Planck equation [6]. In the large-N limit, after integrating over $N - 1$ phases and changing sums to integrals the stochastic differential equation (1) yields the partial differential

 0031-9007/97/78(9)/1616(4)$10.00

equation

$$\frac{\partial P}{\partial t} = -\frac{\partial}{\partial \phi}\Bigg\{\Bigg[-b\sin(3\phi) - \int_0^{2\pi} d\phi' \sin(\phi - \phi')n(\phi',t) + \sigma_M^2 \int_0^{2\pi} d\phi' \sin(\phi - \phi')n(\phi',t)\int_0^{2\pi} d\phi'' \cos(\phi - \phi'')n(\phi'',t)\Bigg]P(\phi,t)\Bigg\} + \frac{\partial^2}{\partial\phi^2}\Bigg\{\Bigg[\sigma_A^2 + \sigma_M^2\bigg(\int_0^{2\pi} d\phi' \sin(\phi - \phi')n(\phi',t)\bigg)^2\Bigg]P(\phi,t)\Bigg\}, \tag{3}$$

with the probability distribution $P(\phi,t)$ of ϕ_i at time t in Stratonovich interpretation. In Eq. (3) $n(\phi,t)$, the normalized number density of the oscillators with phase ϕ at time t, is given by $n(\phi,t) = \sum_{i=1}^{N}\delta(\phi_i(t) - \phi)/N$. Since Eq. (3) has a closed form in ϕ with integrations of $n(\phi',t)$ multiplied by $\sin\phi'$ and $\cos\phi'$ over ϕ', ϕ_i's are statistically independent, and thus, $n(\phi,t)$ may be identified with $P(\phi,t)$. In this paper we analyze the steady state probability distribution $P(\phi)$ achieved as $t \to \infty$.

Since Eq. (3) is invariant under the global inversion we can assume $P(\phi)$ as an even function, i.e., $P(-\phi) = P(\phi)$ restricting the system within the ergodic component including the state $\phi_i = 0$ for all i. This symmetry is confirmed by extensive numerical simulations. One can obtain $P(\phi)$'s of the other ergodic components by the global translation operation (2). With this assumption the stationary probability distribution is written as

$$P(\phi) = Z^{-1}\exp(-\gamma\cos\phi)(1 + A\cos\phi)^{\beta-1/2} \times (1 - A\cos\phi)^{-\beta-1/2}, \tag{4}$$

where

$$\beta = \frac{(\Delta + 3b)\sigma_M^2\Delta^2 + 4b\sigma_A^2}{2\sigma_M^2\Delta^2\sqrt{\sigma_A^2 + \sigma_M^2\Delta^2}},$$

$$\gamma = \frac{4b}{\sigma_M^2\Delta^2},$$

$$A = \frac{\sigma_M\Delta}{\sqrt{\sigma_A^2 + \sigma_M^2\Delta^2}},$$

with a normalization constant Z given by $\int_0^{2\pi} P(\phi)\,d\phi = 1$ and a self-consistent equation

$$\Delta = \int_0^{2\pi}\cos\phi P(\phi)\,d\phi \equiv f(\Delta). \tag{5}$$

When $\Delta = 0$, Eq. (4) has the translational symmetry (2) leading to $P(\phi) = \exp[b\cos(3\phi)/3\sigma_A^2]/Z$, and nonzero Δ gives the symmetry-breaking states related by the translation operation (2). Thus, Δ plays a role of an order parameter for the translational symmetry. Figure 1 shows $P(\phi)$ for the symmetric and the asymmetric states. For small Δ expanding $P(\phi)$ as a power series of Δ we obtain the self-consistent equation (5) as

$$\Delta = \frac{\Delta}{2\sigma_A^2} + \frac{5C_1 + (5bC_0 + bC_2 + 5C_1\sigma_A^2)\sigma_M^2}{40\sigma_A^2 C_0} \times \Delta^2 + O(\Delta^3), \tag{6}$$

with $C_\mu = \int_0^{2\pi}\cos(\mu\phi)\exp(b\cos\phi/3\sigma_A^2)\,d\phi$. While for small σ_A Eq. (5) gives a solution of nonzero Δ, for large σ_A it has only a solution $\Delta = 0$. This implies that there is a transition from a symmetric ($\Delta = 0$) state to a symmetry-breaking ($\Delta \neq 0$) state at a critical noise intensity σ_{Ac}. If the transition is continuous, then the critical noise intensity is given by $\sigma_{Ac} = 1/\sqrt{2}$ [5]. The convexity of Eq. (6) for small Δ, however, gives the possibility of first-order transition.

Figure 2 shows $\Delta - f(\Delta)$ zeros of which are solutions of self-consistent equation (5). When $\sigma_M = 0$ and $b = 1$, Fig. 2(a) shows the discontinuous transition. For $\sigma_A < \sigma_{Ac0} = 1/\sqrt{2}$, there are two zeros of $\Delta - f(\Delta)$; one is zero and the other is nonzero. Since the slope of $\Delta - f(\Delta)$ at $\Delta = 0$ is negative, $\Delta = 0$ is an unstable solution of Eq. (5). Thus when $\sigma_A < \sigma_{Ac0}$, the system is on a symmetry-breaking ($\Delta \neq 0$) state. For $\sigma_{Ac0} < \sigma_A < \sigma_{Ac1} \equiv 0.7111$ there are three zeros of $\Delta - f(\Delta)$ with stable symmetric ($\Delta = 0$) and symmetry-breaking ($\Delta \neq 0$) states implying multistability. For $\sigma_A > \sigma_{Ac1}$ there is only a solution $\Delta = 0$ representing a symmetric state. The effect of fluctuating interaction on the system

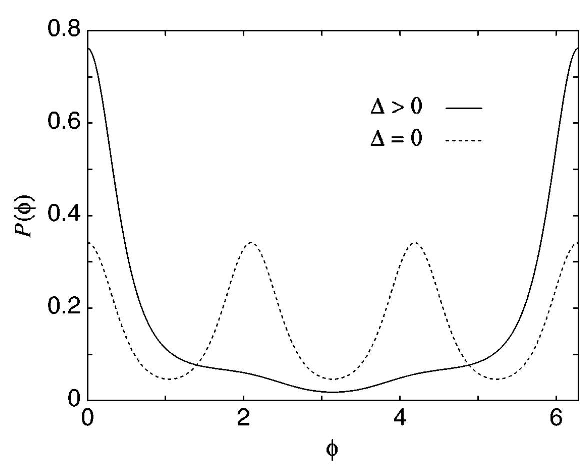

FIG. 1. Schematic diagram of $P(\phi)$ for the symmetric ($\Delta = 0$) state and the asymmetry ($\Delta > 0$) state.

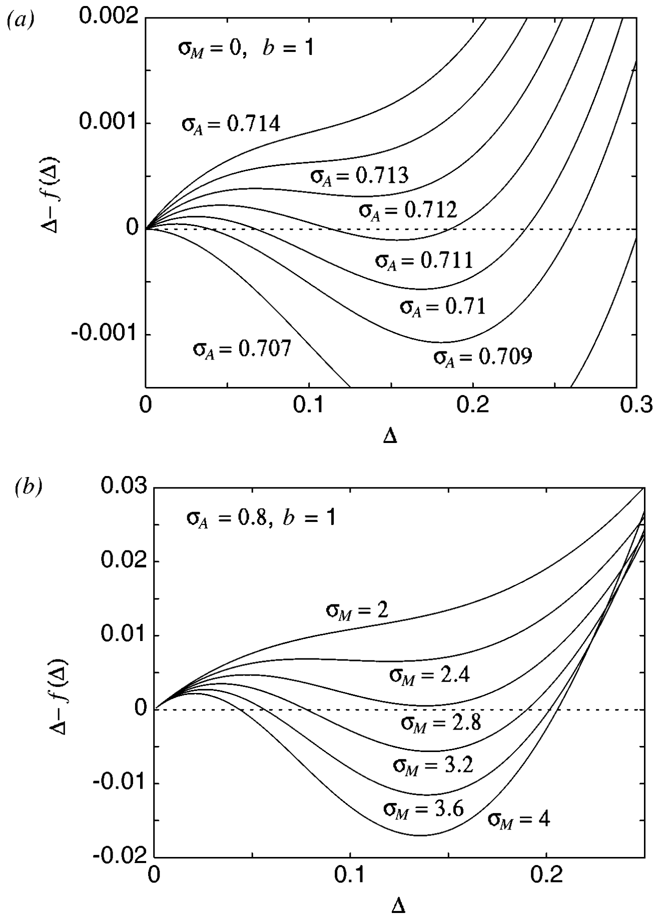

FIG. 2. Plots of $\Delta - f(\Delta)$ versus Δ (a) for various values of σ_A with $\sigma_M = 0$ and $b = 1$, and (b) for various values of σ_M with $\sigma_A = 0.8$ and $b = 1$.

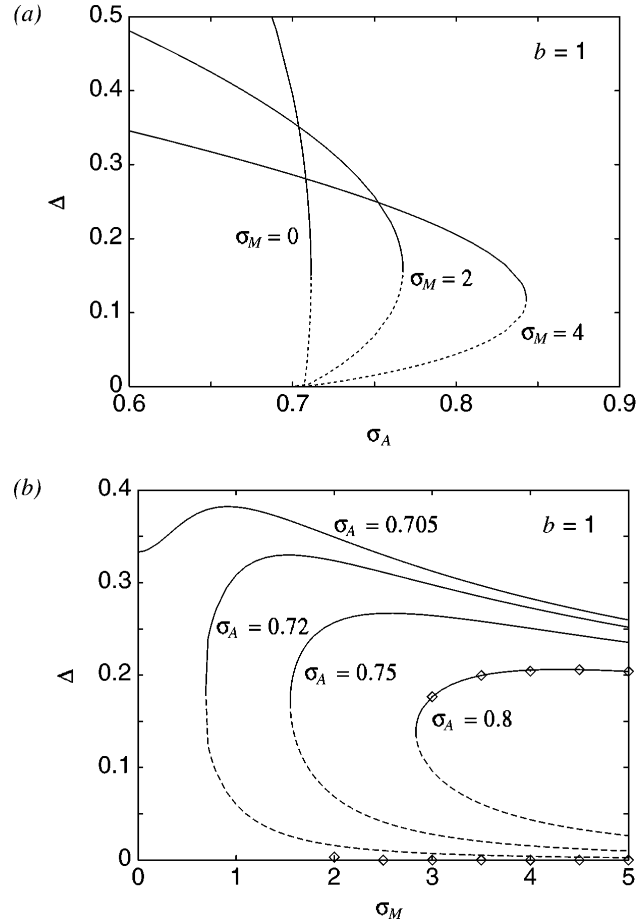

FIG. 3. Plots of Δ obtained from the self-consistent equation (5) (a) versus σ_A for various values of σ_M with $b = 1$, and (b) versus σ_M for various values of σ_A with $b = 1$. Solid and dashed lines represent stable and unstable solutions, respectively. ◇'s indicate Δ in steady state obtained from the numerical simulation for the system of size $N = 10^4$ at $\sigma_A = 0.8$ and $b = 1$.

is shown in Fig. 2(b) at $\sigma_A = 0.8$ and $b = 1$. While for $\sigma_M < \sigma_{Mc} \equiv 2.9$, $\Delta - f(\Delta)$ has only a solution $\Delta = 0$ representing a symmetric state, for $\sigma_M > \sigma_{Mc}$ it has three solutions, two stable and one unstable, implying the multistability of symmetric and symmetry-breaking states.

Figure 3(a) shows the solutions of the self-consistent equation (5) as a function of σ_A for various values of σ_M. For small σ_A there are two solutions $\Delta = 0$ and Δ_s [solid line in Fig. 3(a)]. While $\Delta = 0$ is an unstable solution, $\Delta_s \neq 0$ is a stable solution. As σ_A increases up to σ_{Ac0} the stabilities of the solutions persist reducing Δ_s. At $\sigma_A = \sigma_{Ac0}$, a saddle-node bifurcation occurs changing the stability of $\Delta = 0$ from an unstable state to a stable state and producing an unstable nonzero solution Δ_u [dashed line in Fig. 3(a)] at $\Delta = 0$. As σ_A increases further up to σ_{Ac1}, Δ_u increases and Δ_s decreases. Δ_u and Δ_s meet together at $\sigma_A = \sigma_{Ac1}$ leading to an inverse saddle-node bifurcation. For $\sigma_A > \sigma_{Ac1}$ there is only a stable solution $\Delta = 0$ implying a symmetric state.

Figure 3(b) shows the solutions of self-consistent equation (5) as a function of σ_M for various values of σ_A. For $\sigma_A < \sigma_{Ac0}$ [$\sigma_A = 0.705$ in Fig. 3(b)], there are two solutions $\Delta = 0$ and Δ_s [solid line in Fig. 3(b)] for all values of σ_M; while $\Delta = 0$ is an unstable solution, $\Delta_s \neq 0$ is a stable solution. When $\sigma_A > \sigma_{Ac0}$, for small σ_M there is only a stable solution $\Delta = 0$. At $\sigma_M = \sigma_{Mc}$ the stability of $\Delta = 0$ changes from an unstable state to a stable state and the saddle-node bifurcation occurs at finite Δ producing a stable and an unstable solutions, Δ_s [solid line in Fig. 3(b)] and Δ_u [dashed line in Fig. 3(b)], respectively. As σ_M increases above σ_{Mc} up to some value of σ_M, σ_{M0}, Δ_s increases and Δ_u decreases. At $\sigma_M = \sigma_{M0}$ Δ_s has a maximum value, and as σ_M increases further Δ_s also decreases. In Fig. 3(b) we also show the numerical simulation result consistent with the analytical one at $\sigma_A = 0.8$.

Figure 4 shows phase diagrams in the σ_M-σ_A plane for various values of b. For all σ_M, there are two transition points σ_{Ac0} and σ_{Ac1} at which the transitions from the symmetry-breaking phase (BS) to the multistable phase (MS) and from the multistable phase to the symmetric phase (S), respectively, occur. While in the S phase with

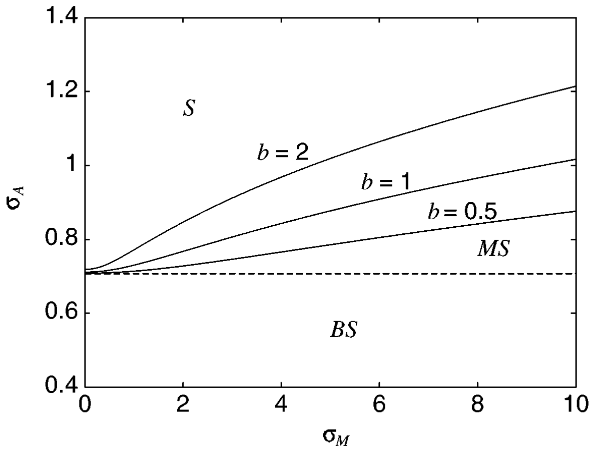

FIG. 4. Phase diagrams in the σ_M-σ_A plane for various values of b. S, BS, and MS represent symmetric, symmetry breaking, and multistable phases, respectively.

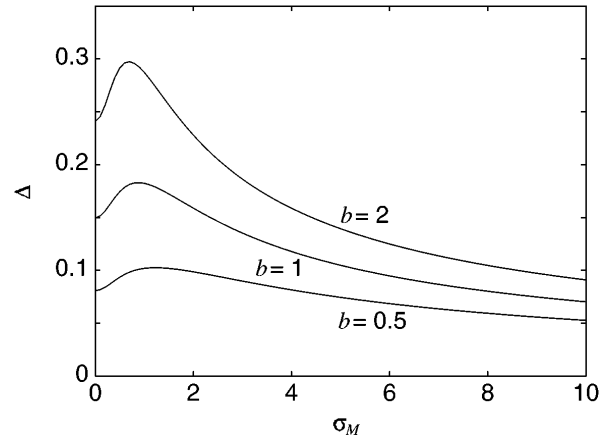

FIG. 5. Plots of jump values of Δ at transition points versus σ_M for various values of b.

$\Delta = 0$ the phase space is ergodic as a whole, in the BS phase with $\Delta \neq 0$ the phase space divides into the three ergodic components related by the translation operation (2). In the MS phase there are four ergodic components, one symmetric component with $\Delta = 0$ and three asymmetric components with $\Delta \neq 0$. The asymmetric components are also related by the translation operation (2). Thus, in the MS phase symmetric and asymmetric components coexist.

The transitions are subcritical saddle-node bifurcations. As σ_M increases, σ_{Ac1} increases with constant σ_{Ac0} expanding the multistable phase. While when $\sigma_M = 0$ the multistable region is $\sigma_A \in (0.707, 0.711)$, when $\sigma_M = 10$ it is $\sigma_A \in (0.707, 1.017)$ expanded 77.5 times. The fluctuating interaction enhances the multistable region drastically. In Fig. 5 we show the jump of stable solution Δ of Eq. (5) at the transition point σ_{Ac1}. At $\sigma_M = 0$ the jump is finite implying the discontinuous transition. As σ_M increases up to some value of σ_M, σ_{Mp} the jump increases, and as σ_M increases further it decreases showing a peak and implying the maximum discontinuity at σ_{Mp}.

In conclusion, we have investigated the nonequilibrium phase transition of globally coupled oscillators with a third harmonic pinning force in the presence of additive and multiplicative noises. It has been shown that the noises induce a subcritical saddle-node bifurcation from an asymmetric state to a symmetric state at a critical noise intensities leading to the multistability. The multistability has been enhanced drastically by the multiplicative noise. Discontinuity of the transition is maximized at finite multiplicative noise intensity. This noise-enhanced multistability comes from the role of the multiplicative noise that it reduces the fluctuation intensity, $\sum_{j=1}^{N} \sin(\phi_i - \phi_j) = \Delta \sin \phi_i$ in the Langevin equation (1). Since $\Delta = 0$ in the symmetric state and $\phi_i = 0$ for all i in the synchronized (symmetry-breaking) state, the fluctuation intensity is zero in both states. Thus the multiplicative noise tends to stabilize both symmetric and synchronized states enhancing the multistability.

This work has been supported by the Ministry of Information and Communication, Korea. We are grateful to Dr. E. H. Lee for his support on this research.

*Electronic address: skim@logos.etri.re.kr

[1] C. Van den Broeck, J. M. R. Parrondo, J. Armero, and A. Hernández-Machado, Phys. Rev. E **49**, 2639 (1994); C. Van den Broeck, J. M. R. Parrondo, and R. Toral, Phys. Rev. Lett. **73**, 3395 (1994).
[2] S. H. Park and S. Kim, Phys. Rev. E **53**, 3425 (1996).
[3] S. Kim, S. H. Park, and C. S. Ryu, ETRI J. **18**, 147 (1996); S. Kim, S. H. Park, C. R. Doering, and C. S. Ryu, Phys. Lett. A (to be published).
[4] A. Fulinski and T. Telejko, Phys. Lett. A **152**, 11 (1991).
[5] S. Kim, S. H. Park, and C. S. Ryu, Phys. Rev. E **54**, 6042 (1996).
[6] H. Risken, *The Fokker-Planck Equation* (Springer-Verlag, New York, 1988).